







Bridging Human-Robot Co-Adaptation via Biofeedback for Continuous Myoelectric Control

Xuhui Hu , Member, IEEE, Aiguo Song , Senior Member, IEEE, Hong Zeng , Member, IEEE, Zhikai Wei , Hanjie Deng , and Dapeng Chen , Member, IEEE

Abstract—This letter proposes a novel human-robot co-adaptation framework for robust and accurate user intent recognition, specifically in the context of automatic control in assistance robots such as neural prosthetics and rehabilitation devices empowered by electrophysiological signals. Our goal is to incorporate user adaptability early in the training phase to facilitate both machine recognition and user adaptability, rather than relying solely on brute-force machine learning methods. The proposed framework is featured by applying biofeedback-based user adaptive behavior into model training, while the machine can adapt to those changes through online learning. Specifically, this study focuses on the recognition of two-degree-of-freedom simultaneous and continuous wrist movement intentions based on surface electromyogram (sEMG) array signals, and the performance is tested on twelve able-bodied subjects. The co-adaptive evaluation experiment demonstrates the robust control of this method by introducing sEMG electrode displacement as perturbations. Experimental results show that this method improves the completion time of centre-out tasks by 13% compared to conventional methods (Cohen's $d = 0.637$), and debias 86% of the effect of electrode shift perturbations. This study provides insights into the potential for incorporating human adaptability into machine intelligence to improve user intent recognition and automatic robot control.

Index Terms—Human-robot co-adaptation, myoelectric control, EMG, user intent recognition.

I. INTRODUCTION

DECODING user intent based on electro-physiological signals, then controlling assistance robots, such as neural

Manuscript received 10 July 2023; accepted 25 October 2023. Date of publication 3 November 2023; date of current version 15 November 2023. This letter was recommended for publication by Associate Editor V. Vashista and Editor P. Valdastrì upon evaluation of the reviewers' comments. This work was supported in part by the CEC-Tencent Robotics X Rhinoceros Bird Special Research Program Project and in part by the National Natural Science Foundation of China under Grants 92148205, 62173089, 61673105, and 62003169. (Corresponding author: Aiguo Song.)

This work involved human subjects or animals in its research. Approval of all ethical and experimental procedures and protocols was granted by the Ethics Committee of Jiangsu Province Hospital under Application No. 2020-SR-362, and performed in line with the Declaration of Helsinki.

Xuhui Hu, Aiguo Song, Hong Zeng, Zhikai Wei, and Hanjie Deng are with the State Key Laboratory of Digital Medical Engineering and Jiangsu Key Laboratory of Remote Measurement and Control, School of Instrument Science & Engineering, Southeast University, Nanjing, Jiangsu 210096, China (e-mail: xuhui.hu@seu.edu.cn; a.g.song@seu.edu.cn; hzeng@seu.edu.cn; 230228933@seu.edu.cn; hj.deng@siat.ac.cn).

Dapeng Chen is with the School of Automation, Nanjing University of Information Science & Technology, Nanjing, Jiangsu 210044, China (e-mail: dpchen@nuist.edu.cn).

This letter has supplementary downloadable material available at <https://doi.org/10.1109/LRA.2023.3330053>, provided by the authors.

Digital Object Identifier 10.1109/LRA.2023.3330053

prosthetics and rehabilitation devices, is an ideal solution for intuitive control by disabled persons such as amputees [1] stroke victims [2], and paralyzed individuals [3]. However, the robustness of intent recognition based on electroencephalogram (EEG) and surface electro-myogram (sEMG), has always been a challenge for researchers due to the instability during signal acquisition [4], [5], [6], the non-stationary randomness of the signal itself [7], and differences in physiological characteristics among individuals [8], [9], all of which may cause feature drift, making it difficult for users to control robots with stability [10], [11], [12].

In a recent study, He et al. [13] found that user adaptation can effectively alleviate sEMG feature drift. This discovery has prompted researchers to reconsider that rather than relying solely on brute-force machine calculations to approach the limits of user intent recognition, could we instead adopt a more user-centered strategy by helping users adapt to machines? For this reason, Barradas et al. [14] proposed the EMG space similarity feedback to improve the consistency of users' muscle synergy features. Fang et al. [15] introduced a clustering feedback strategy that provides users with real-time bio-feedback by visualizing the online sEMG signal input and the centroids of the training samples. The results show that the final online recognition accuracy exceeds the prior offline accuracy evaluated during model calibration.

The routine training-and-testing protocol, which is well-established in various machine learning based applications, also dominates in current human-robot control studies [16]. However, there are certain limitations in effectively integrating human adaptability with machine intelligence within such a protocol. The challenges primarily stem from the methodologies employed for constructing the training set and optimizing the intent decoding model. To clarify this statement, consider three common training set acquisition methods in myoelectric applications, i.e., visual cue training [17], mirror training [18] and unsupervised pre-calibration training [19]. These methods pose difficulties for users to confirm whether their intended gestures align with the labeled gestures due to the lack of real-time feedback during data acquisition. This issue becomes especially pronounced when attempting to label continuous and simultaneous gestures. As a compromise, most training methods are limited to label the gestures of single-degree-of-freedom [17], [19].

Users are required to passively generate movements according to instructions, but cannot receive the feedback from the machine, thereby this phase is usually considered as an open-loop

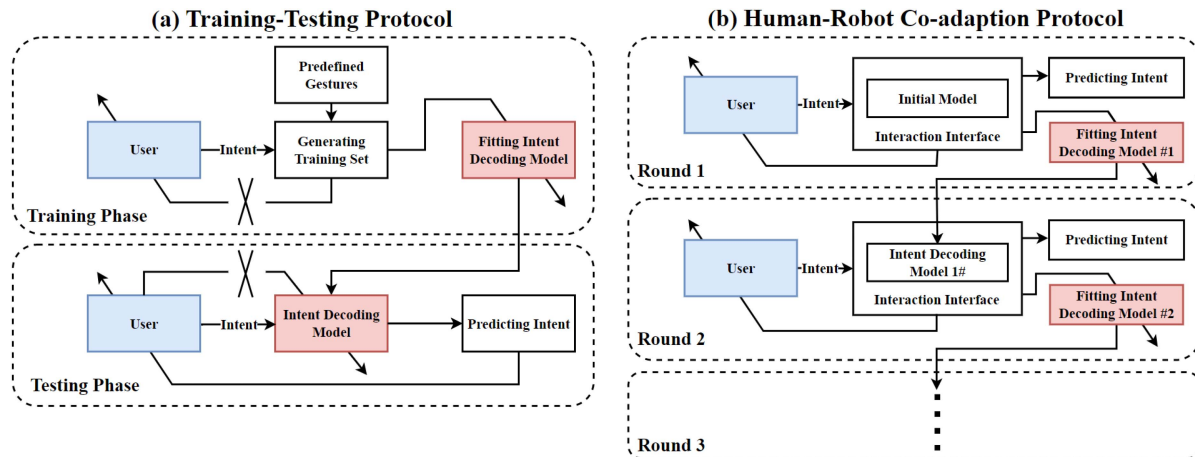


Fig. 1. Framework of (a) the training-testing protocol versus (b) the human-robot co-adaptation protocol.

calibration, where without the feedback the user's adaptability is essentially excluded from the training set. In the testing phase, while human adaptability can be fully engaged by multiple biofeedback methods [14], [15], [20], it only makes people more adaptable to the trained model, the myoelectric control model itself does not integrate adaptability. As a result, machine intelligence and user adaptability are isolated in the training and testing phases respectively. Recently, Fang et al. [21] proposed an adaptive accelerated learning algorithm to aggressively compress and update the intent decoding model in response to different inputs. Moin et al. [22] used hyper-dimensional computing to implement in-sensor adaptive learning and real-time inference for hand gesture classification. These work aims to investigate how to make the machine adapts to the user.

A more effective optimization process for human-machine systems would be a bidirectional spiral of machine intelligence and human adaptability. Such co-adaptive methodologies have been increasingly used in myoelectric control, with researchers proposing both supervised and unsupervised approaches. In the supervised approach proposed by Hahne et al. [17], the machine detects errors during intent recognition and updates the model using recalibration data to incorporate user adaptability into model training. Yeung et al. [23] proposed an unsupervised approach based on non-negative matrix factorization (NMF) that allows for seamless updates of real-time myoelectric control. Nevertheless, these studies still use traditional open-loop calibration methods before incorporating user adaptability into model fitness. Therefore, one of the goals of this letter is to investigate whether human adaptability can be involved into the training process beforehand to facilitate both machine recognition and user adaptability.

In this letter, we present a human-robot co-adaptation framework featured by applying biofeedback-based user adaptive behavior into model training, while the machine can adapt to those changes online. Through incorporating user intent related biofeedback into the training phase, the user adaptability is involved earlier for model fitness. we take the myoelectric control interface as an entry point and aim to recognize two-degree-of-freedom (2-DOF) simultaneous and continuous motion intent

of the wrist based on sEMG array signals. In the myoelectric control experiment, we test the performance on twelve able-bodied subjects. In order to clearly assess the contribution of human adaptation and machine adaptation in this system, we specifically design a co-adaptive evaluation experiment to demonstrate the control robustness against disturbance quantities, which is simulated by introducing electrode shift of sEMG array sensors. Finally, we compare the results with the conventional training methods to highlight the potential implications as well as the inherent limitations associated with the study.

II. METHODS

A. Human-Robot Co-Adaptation Training Framework

To begin with, the comparison between the traditional training-and-testing protocol and the proposed co-adaptation protocol is shown in Fig. 1, where users and machines are presented as two objects with adjustable parameters in the control loop and denoted by red and blue blocks, respectively. In Fig. 1(a), users need to perform actions consistent with the preset gesture instructions during the training phase to form a training set. However, this process is considered as open-loop because users cannot obtain feedback information to actively adjust possible myoelectric feature drifts. After collecting multiple rounds of the data, this training set will be used to complete the fitting between input features and user intent labels. Then, the model will go through testing phase where the user inputs sEMG signals into the trained model and outputs the control signals. Although the user can utilize model output as feedback, the fixed model parameters limit the machine's adaptability to the user. As a result, the adaptability of the machine and the user is separated in the training and testing phases, both of them have only taken one step towards the optimal level without forming co-adaptation.

This letter introduces a novel co-adaptation paradigm based on closed-loop training data collection and online decoding model updates, as shown in Fig. 1(b). Generally, it involves the following iterative steps:

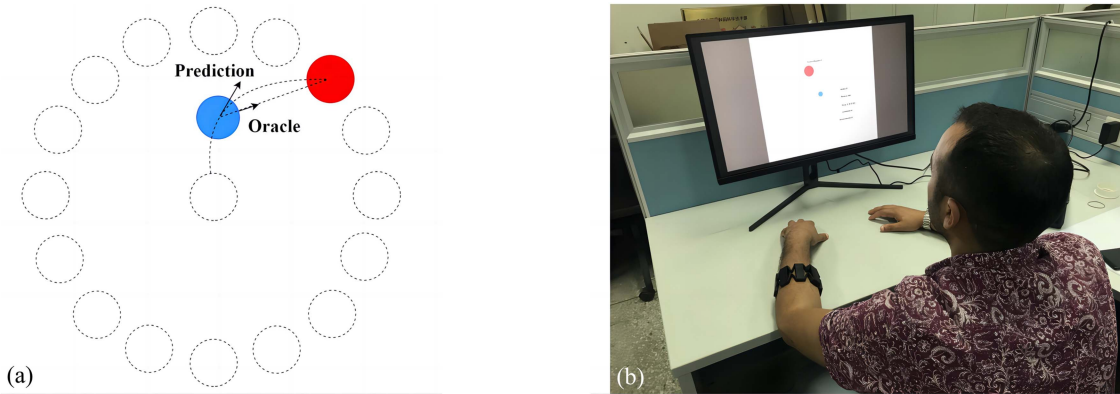


Fig. 2. (a) Interface of the two-dimensional centre-out task. (b) The experimental setup for the myoelectric control interface.

- 1) **Interactive Data Collection:** New data is collected from both the user and the machine through an interactive interface, where the user can perform myoelectric control and receiving biofeedback simultaneously. This interface facilitates the exchange of information between the two entities, forming a bidirectional closed loop.
- 2) **Model Training and Updating:** The collected data is then used to update the training set, which is utilized to fit a new intent recognition model. This updated model enhances the system’s ability to accurately interpret and understand user inputs.
- 3) **Control Strategy Update:** The newly fitted model is employed to update the control strategy of the interface. This ensures that the interface becomes more adept at responding to user inputs by incorporating the insights gained from the updated model.
- 4) **Iterative Process:** The system then enters a cyclical process, returning to step 1) where new data is collected based on the refined control strategy. The iterative nature of this process allows for continuous adaptation and improvement of the system’s performance over time.

Unlike visual-cue training, this method allows the user to actively interact with the machine during the data collection phase, thus the user’s active adaptability is stored in the training set. In summary, this paradigm fuses human adaptability with myoelectric control by introducing bio-feedback in an interactive interface, and through iteratively updating the intent recognition model, the machine can also adapt to users. Eventually, this framework contributes to a bidirectional spiral of machine intelligence and human adaptability.

B. Continuous Myoelectric Control Interface

In this subsection, we will expound on the co-adaptation framework for 2-DOF continuous myoelectric control of the wrist. First, a two-dimensional centre-out cursor task under continuous myoelectric control is designed, as shown in Fig. 2(a). It is through such an interactive task that enables closed-loop sEMG acquisition, where the sEMG array sensors set around the user’s forearm to implement the myoelectric control interface (as shown in Fig. 2(b)). In this task, the user’s goal is to control a blue

cursor in the center of the screen to hit a red target that appears in one of 16 evenly distributed positions around the cursor. Each round of the centre-out cursor task consists of 16 trials, with the target appearing once in each direction in a pseudo-random order. The user needs to complete each trial as quickly as possible by conducting the wrist flexion/extension (horizontally movement of the cursor) or wrist adduction/abduction (vertically movement of the cursor). Each trial is set to complete within five seconds to avoid unnecessary time waste.

The Multi-Layer Perceptron (MLP) is a classical neural network architecture used to solve classification or regression problems. Using this model ensures that any improvements come primarily from the co-adaptation method and not from the influence of the neural network itself. Once the MLP performs well, there is more confidence in applying more complex neural networks. Here, the MLP is used to control the velocity of the cursor movement by taking eight-channel sEMG signals as input and outputting two continuous predictions for horizontal and vertical motion speed. The hidden layer of MPL contains 50 neurons with a Rectified Linear Units (ReLU) as activation functions. Finally, ADAM optimizer with a learning rate of 0.001 was used for model fitting. To ensure fit quality, the amplitude of both input features and motion intent labels were normalized to the range of [0,1].

Correct data labeling of EMG feature is crucial for myoelectric control. Meanwhile, the pre-calibration (e.g. as adopted by Jiang [19] or Hahne [17]) during the training phase may be insufficient to adapt to potential changes during online control. Therefore, the idea solution to this problem is to accurately label the user’s intent online. Inspired by the idea of “supervised recalibration” based on the Brain-Machine Interface study by Gilja et al. [24], we use the knowledge of the target and cursor in the interactive interface to infer the user intent.

Specifically, Gilja et al. [24] introduce a method called “oracle intent”, which assumes that users always seek to move straight to the target from wherever the cursor is. Therefore, the ground-truth user intent (i.e. oracle intent) was formed by rotating the cursor decoded online (denoted as “Prediction” in Fig. 2(a)), so that the velocity direction of the cursor is pointed straight at the target (denoted as “Oracle” in Fig. 2(a)) [7]. As is shown in (1), $\hat{h}_{y_{oracle}}$ is a unit vector denoting the direction of the oracle

intent, x_{target} and x_{cursor} denotes target position and cursor position in the coordinate system of the interface. However, the previous studies only defined the cursor's motion as a unit vector, i.e. the cursor always moves at a uniform speed, so we further optimized the above method to modulate cursor velocity as the linear function of the sEMG array activation signals, which have been adopted in our previous work [9], [25]. As is shown in (2), we characterize the scaled value of the cursor speed in terms of the algebraic sum of the root mean square (RMS) of the sEMG array signals. Given bins of sEMG data and simultaneous oracle intent, the parameters of the MLP could be updated in a supervised fashion.

$$\hat{y}_{oral} = \frac{x_{target} - x_{cursor}}{\|x_{target} - x_{cursor}\|} \quad (1)$$

$$y_{oral} = \sum_{i=1}^8 RMS_i \cdot \hat{y}_{oral} \quad (2)$$

In summary, we use ‘‘oracle intent’’ to annotate user movement (including motion direction and speed) in real-time during centre-out tasks. Therefore, the collected data includes adaptive features of users to cope with unintended cursor dysfunction, realizing a closed-loop data collection for the training set. After each round of data collection, the MLP model learns from the training set and use the updated parameters for the next round of myoelectric control. As a result, both machine adaptation and user adaptation are utilized and mutually optimized towards an optimal level.

C. Experimental Process Design

Twelve able-bodied participants ($26\hat{\pm}3$ years old) were recruited to perform an online myoelectric control experiment, each participant read and signed an informed consent form before proceeding with the experiments. The experimental protocol was approved by the Ethics Committee of Jiangsu Province Hospital (2020-SR-362). All experiments were conducted according to the ethical guidelines for medical research involving human participants (according to the Declaration of Helsinki). The experiment consists of two parts: Firstly, in order to evaluate the proposed method in terms of human-machine co-adaptation, including the impact on perturbations and on the user's learning effect, we referred to Couraud et al. [26] and designed a co-adaptation evaluation experiment. Then, we further designed a controlled experiment to compare the differences between the present approach and the traditional training-testing approach. Throughout the experiments, MYO Armband (Thalmic Lab) is adopted for sEMG array signal acquisition, with root mean square value (RMS) used as the input feature of the MLP model. Participants were seated calmly in a chair with their upper arms relaxed and their forearms at a 90-degree angle with support at the wrist.

All the participants perform the co-adaptation evaluation experiment at first, which consists of three phases, namely ‘‘Baseline’’, ‘‘Co-adaptation’’ and ‘‘Post-effect’’, as shown in the Fig. 3, where the user is required to use co-adaptive method to complete the following three sessions in turn:

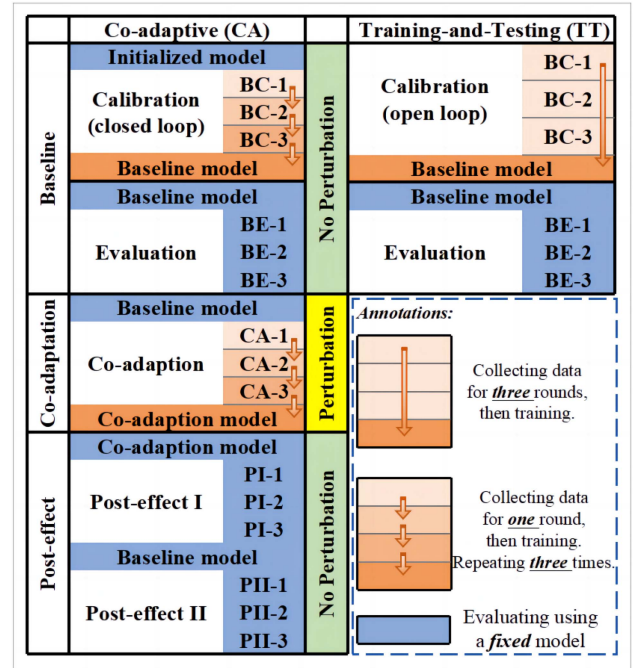


Fig. 3. Sequence of co-adaptation evaluation experiment.

- 1) ‘‘Baseline’’ phase: the user starts the interaction task under initial experimental conditions, where the initial parameters of the model are randomly given. The user updates the interaction experiment through three iterations (denoted as BC-1, BC-2 and BC-3) to form a baseline myoelectric control model. The parameters of the fixed model were then used as the baseline model and the performance of the baseline was evaluated through three rounds of experiments (denoted as BE-1, BE-2 and BE-3).
- 2) ‘‘Co-adaptation’’ phase: We refer to Yeung et al. [23] by introducing an electrode offset perturbation in order to test the adaptability to model changes. In this phase, the MYO armband is rotated transversally such that the sensor pod was shifted closer to the medial epicondyle by the distance of one pod, then the subject is asked to complete three iterations of the centre-out tasks based on the baseline model. In the first round, the machine has not yet been adapted to the user's movements (as shown in Fig. 1(b), ‘‘Round 1’’), so the solely user adaptability can be evaluated. In the next two rounds, the machine learns from the accumulated user adaptation data, allowing for evaluating the co-adaptability between the user and machine. If the model converges as the number of training rounds increases, it can be concluded that the model is able to adapt to the perturbation.
- 3) ‘‘Post-effect’’ phase: the perturbation is removed and co-adaptation is turned off. This phase is divided into six rounds, with the first three rounds using a fixed ‘‘Co-adaptation model’’ learned in the previous ‘‘Co-adaptation’’ phase to assess whether this model not only adapts to the perturbation, but also maintains good control robustness after the perturbation is removed. In the last three rounds, a fixed ‘‘Baseline model’’ trained in the

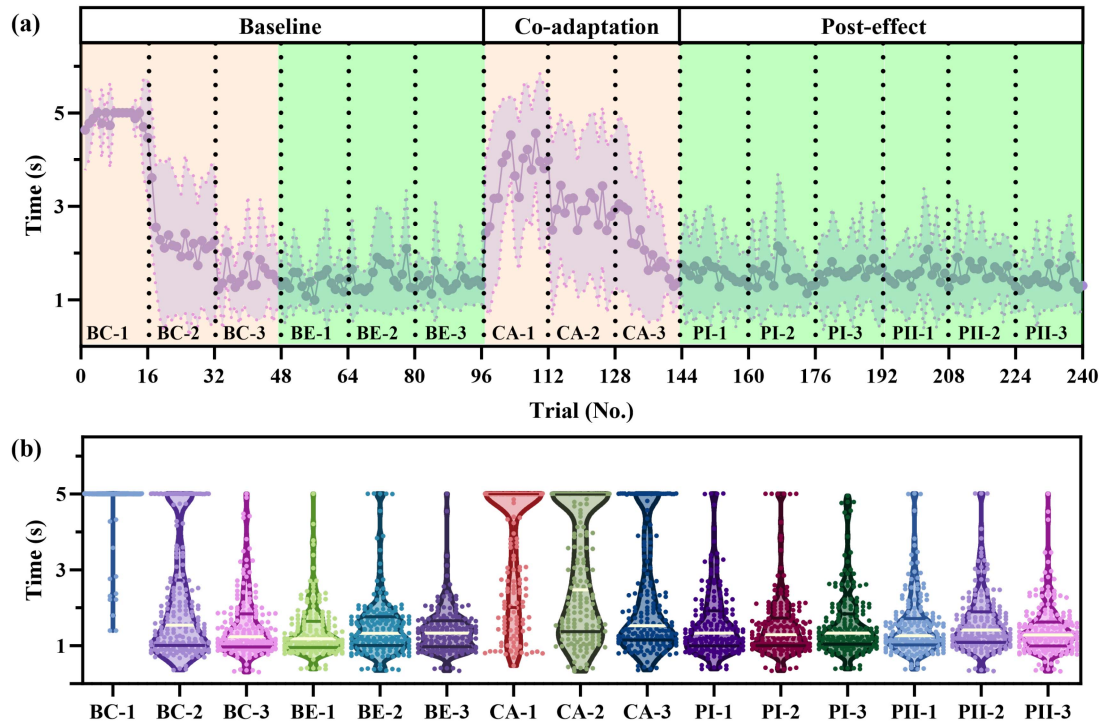


Fig. 4. (a) Learning curve of the co-adaptation evaluation experiment. (Tips: the learning phase is marked with orange areas and the non-learning phase is marked with green areas). (b) Boxplot of the task completion time on each experimental group.

“Baseline” phase (the same model used in BE-1 to BE-3) is used to assess whether the user still performs as well as it did before after a number of co-adaptation trials, and if not, it would indicate that the user had been molded to be more attuned to the “co-adaptation model”.

Secondly, we set up a control group using the traditional training-and-testing framework to make a fair comparison with co-adaptation method on the same interaction task. All the subjects participated in the experiment without muscle fatigue. We only compare them in the baseline phase because assessing the impact of perturbations on traditional models may not be meaningful, as the model performance is usually sensitive to perturbations. In the control group, the myoelectric control model was trained based on three rounds of open-loop data acquisition, then the model is evaluated for three rounds of center-out experiments. The training method for this control group is based on our previous research [9], [25], which is designed to match sEMG signals with continuous movement intent of users, and then applied a training-testing framework for model fitting.

D. Evaluation Metrics and Statistic Analysis

Task completion time and path tracking error are effective metrics for evaluating the interaction performance. In this experiment, we use these two metrics to comprehensively evaluate the participants’ performance. The path tracking error is derived by calculating the root mean square error (RMSE) between the shortest path from the initial cursor position to the target position and the actual cursor path.

To compare the differences between experimental groups, we perform t-test and one-way analysis of variance (ANOVA) with alpha equals to 0.01. To determine if user adaptation was significantly expressed, we perform a one-sample t-test to assess the relationship between task completion time and task sequences. If the slope of the linear regression curve (which represents the change in completion time as task sequence increases) is significantly different from zero, indicating that user adaptation is being expressed. In addition, Cohen’s d is used to quantify the effect size of the difference between two groups.

III. RESULTS

A. Co-Adaptation Evaluation Experiment

Firstly, we illustrate the learning curve of the co-adaptation evaluation experiment (as is shown in Fig. 4(a)), it can be found that:

In the baseline phase, after three rounds of co-adaptive control, the task completion time for the first update compared to the last update was significantly shorter (BC-2 vs. BE-1, $P < 0.001$), showing that the model was converging. There was no significant difference between the completion times of BC-3 and BE-1 ($P = 0.1140$), indicating that the model had completed convergence after two rounds of data collection. In BC-2, the learning curve slope fitted by linear regression is significantly non-zero (Slop = -0.0438 , $F(1,15) = 9.633$, $P = 0.0073$), suggesting that users are adapting to the interface when the decoding model has not been changed.

In the co-adaptation phase, it can be found that the influence of electrode shift is significant (BE-3 vs. CA-1, $P < 0.001$). As

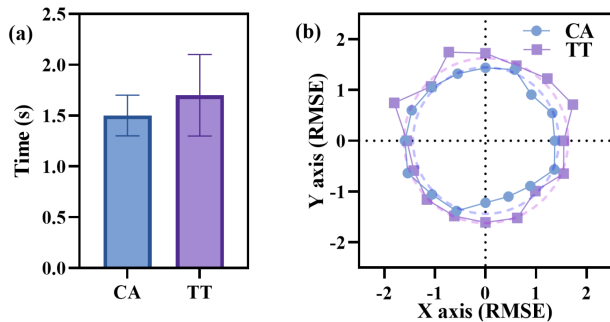


Fig. 5. (a) Box plot of the mean completion time for the experimental group and control group. (b) The cursor tracking path error for 16 targets in the polar coordinate system. (Tips: CA represents co-adaptive method, TT represents training-and-testing method).

CA-1 does not incorporate machine adaptation, it can be found that the users can barely improve the control effect through their own adaptation. However, the task performance improved in the next round, and the final performance returns to the status that without perturbation (BE-3 vs. PI-3, $P=0.0321$), debiasing 86% of the effect of electrode shift perturbations.

In the post-effect phase, the perturbations were removed. However, the completion time for the first three rounds (PI-1 PI-3) showed no significant difference ($F(2,573)=0.3087$, $P=0.7625$), as well as being compared to the case where perturbations were present (CA-3). This suggests that the model did not completely deviate from the initial baseline model in adapting to the perturbations, but rather generalized so that the model is compatible with both the presence and absence of perturbations.

B. Co-Adaptation Versus Training-and-Testing

Section III-A verifies the reliable convergence of the co-adaptation method and tests the model robustness in the presence of perturbations, this subsection compares the proposed method with the traditional Training-and-Testing method. In Fig. 5(a), it shows the box plot of the mean completion time for the experimental group (CA) and control group (TT). The statistical results show that there is a significant difference between CA and TT ($P<0.001$), with CA being 13% faster than TT on average task completion time (CA: 1.51 s; TT: 1.73 s, Cohen's $d=0.637$).

In addition, Fig. 5(b) depicts a visualization of cursor tracking path error for 16 targets in a polar coordinate system. The polar angle is used to represent the direction of the target in the interaction interface (Fig. 2(a)), and the radius of each data point represents the tracking path error of that target. This type of visualization can be useful for identifying any patterns or trends in the tracking errors across different targets, as well as for comparing the magnitude of errors between different targets on the interface. Therefore, the closer the data points are to the origin, indicating the smaller the path error for that target. The dashed circle in this figure indicates the average path error of the experimental group or control group. The results show that the average path error of CA is smaller than that of TT, and the path error of CA is more balanced in all directions.

The reason for the difference in performance probably stems mainly from the data acquisition process: the control group also performed three iterations of data acquisition, but the difference was that the calibration phase only performed open-loop data acquisition for the four directions along the coordinate axes. In contrast, the three rounds of data collection in the experimental group were closed-loop, with the training set containing data in all directions, which was more informative, and each round included information about the user's adaptation, so the results show that the user's adaptation was crucial to the closed-loop data collection of the training data.

C. Trajectory Efficiency

Fig. 6 illustrates the trajectory of the cursor within the interactive interface during each learning phase. The first row shows the co-adaptation process in the baseline stage: in BC-1, the user has no control over the cursor's move to the specified target position as the weights of the intent decoding model are initialized randomly, nevertheless, the user needs to keep the motion intention pointing to the target for helping the machine to acquire the correct user intent; the changes from BC-2 to BE-1 show the process of the machine gradually adjusting the decoding model and improving the myoelectric control performance. The second row of the diagram shows the human-machine learning process during the co-adaptation phase. CA-1 shows the cursor trajectory based on the baseline model (the same model as BE-1) when the electrode shift perturbation is involved, and it can be seen that on the one hand the baseline model is incapable of accurately mapping the user's intention, so that most of the cursor misses the target, and only in a few targets the motion deviations can be compensated by human adaptation, indicating the importance of model updating to accommodate possible perturbations. However, in CA-2, the motion bias has been effectively corrected. CA-3 completes another round of learning with perturbations, while PI-1 removes the perturbations, but the model is based on experimental data from CA-1 to CA-3, and the results show that it still completes the target in all directions successfully, suggesting that the model is compatible with both perturbations and non-perturbations.

IV. DISCUSSIONS AND CONCLUSION

In this letter, we present a human-machine co-adaptive approach, which is characterized not only by incremental learning that allows the machine to continuously update its control model, but also by bidirectional co-adaptive learning between the human and the machine that takes advantage of the flexible adaptability of the human.

Decoding user intent based on electrophysiological signals, thereby controlling assistance robots, typically relies on data-driven methods. These methods involve recording pairs of input feature signals and corresponding user intent labels during the data acquisition phase, followed by fitting a machine learning model in the model training phase. However, the success of machine learning prediction relies heavily on the repetitiveness of the training set data belonging to the same class and the

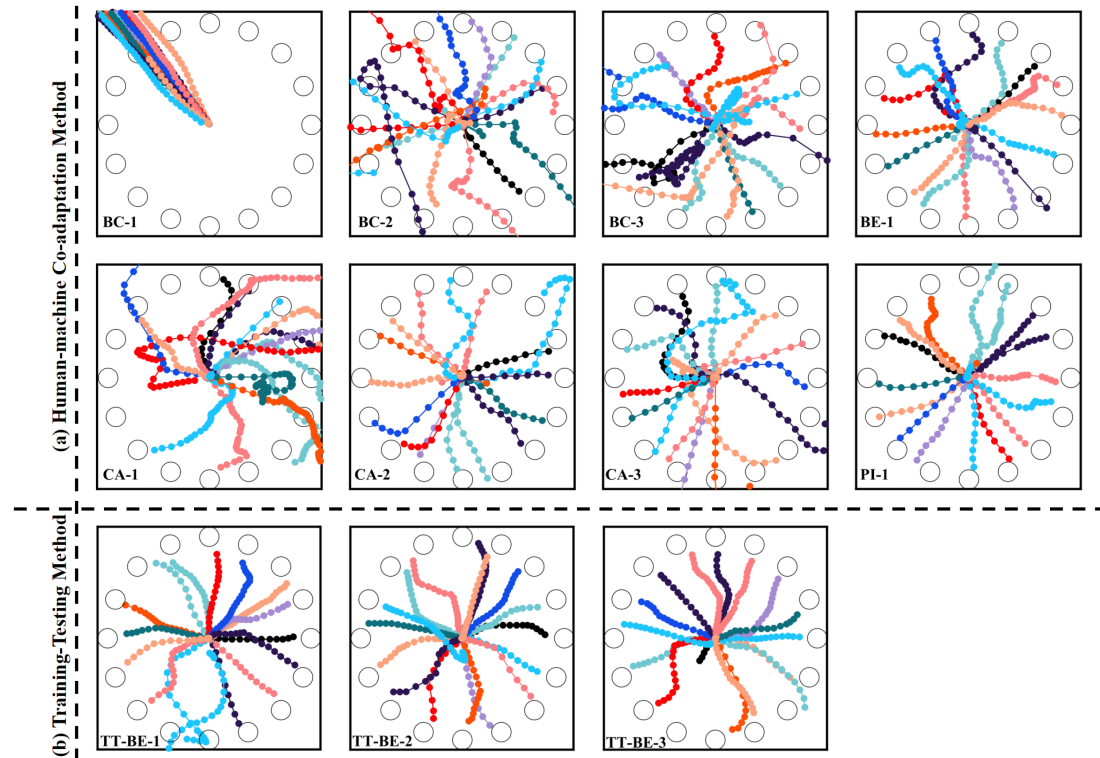


Fig. 6. Trajectory of the cursor within the interactive interface by (a) human-machine co-adaptation method versus (b) training-and-testing method.

significant differences that from the non-related classes. Therefore, the labeling quality of the training set data directly affects the recognition accuracy. As mentioned in Section II-A, the traditional open-loop data collection paradigm has difficulties in confirming whether the underlying motion intentions of the sEMG are consistent with the predefined commands. In contrast, the key features of the proposed method lie in the following aspects: 1) realizing a closed-loop data acquisition by incorporating user adaptation into the training set to improve the quality of training set; and 2) supporting real-time updating which enables the model to withstand possible disturbances and improve the control robustness.

In Section III-A, we dedicated to demonstrate the bidirectional human-machine co-adaptive procedure and the advantages over the conventional training-and-testing protocol. In the co-adaptation evaluation experiments, we visualize the learning procedure and reveal the two key questions for the human-machine co-adaptive system:

- 1) What should people do to promote co-adaptation? This letter demonstrates that the user needs to provide high-quality training data for model fitting in order to make the machine better understand the user's intents. Through closed-loop collection, users can actively adapt their own active motor intentions to the pre-defined labels, thereby improving the quality of the training set data.
- 2) What should machines do to promote co-adaptation? This letter demonstrates that the machine needs to constantly update and converge towards stability in order to adapt to changes that may be caused by the user's own changes or external disturbances.

The post-effect experimental results show that after the model has adapted to the electrode shift, the control accuracy in the unperturbed state is slightly lower than that in the baseline phase. This shortcomings may be due to the fact that after the "co-adaptation" phase, the model training data contains both perturbed and unperturbed cases, and the existing MLP framework is still difficult to achieve a better generalization effect, which makes the co-adaptation model slightly worse than that of the baseline model after the perturbation is removed.

Particularly, the experimental results also show evidence of users adapting to the machine. For instance, the model is fixed in BC-2, but as the trial increases, the completion time appears to decrease ($Slop=-0.0438$, $F(1,15)=9.633$, $P=0.0073$), suggesting that the user is adapting to the current model. Also in PII-1 3, when switching from the co-adaptation model to the baseline model, the user's task completion time also slowly decreases, indicating that the user is gradually adapting to the process of switching from one model to another.

It is worth noting that we will further refine the perturbation evaluation experiments in the future. Specifically, the types of perturbations during human-machine interface can be classified into two categories: one is perturbations from the machine, such as electrode offset (which has been analyzed in this letter); and the other is perturbations from the user, such as EMG feature shifts due to changes in arm posture or load [10, 12, 22]. Therefore, comprehensively analyzing both aspects is of grate significance. In this letter, we mainly concentrate on showing the human-machine co-adaptation process, while in the future we will add detailed analyses on different types of perturbations. Moreover, we will further

reveal whether users adapt their behaviour to the machine, if so, what kind of adaptations would users make. The solution of these questions will help to improve the fundamental research on human-machine co-adaptive mechanisms.

REFERENCES

- [1] J. M. Hahne, M. A. Schweisfurth, M. Koppe, and D. Farina, "Simultaneous control of multiple functions of bionic hand prostheses: Performance and robustness in end users," *Sci. Robot.*, vol. 3, no. 19, 2018, Art. no. eaat3630.
- [2] Z. Lu, K. Y. Tong, X. Zhang, S. Li, and P. Zhou, "Myoelectric pattern recognition for controlling a robotic hand: A feasibility study in stroke," *IEEE Trans. Biomed. Eng.*, vol. 66, no. 2, pp. 365–372, Feb. 2019.
- [3] P. D. Ganzler et al., "Restoring the sense of touch using a sensorimotor demultiplexing neural interface," *Cell*, vol. 181, no. 4, pp. 763–773, 2020.
- [4] X. Hu, A. Song, J. Wang, H. Zeng, and W. Wei, "Finger movement recognition via high-density electromyography of intrinsic and extrinsic hand muscles," *Sci. Data*, vol. 9, no. 1, 2022, Art. no. 373.
- [5] J. L. Segil, R. Kaliki, J. Uellendahl, and R. F. Ff Weir, "A myoelectric postural control algorithm for persons with transradial amputations: A consideration of clinical readiness," *IEEE Robot. Autom. Mag.*, vol. 27, no. 1, pp. 77–86, Mar. 2020.
- [6] M. Han, M. Zandigohar, M. P. Furmanek, M. Yarossi, G. Schirmer, and D. Erdogmus, "Classifications of dynamic EMG in hand gesture and unsupervised grasp motion segmentation," in *Proc. 43th Annu. Int. Conf. IEEE Eng. Med. Biol. Soc.*, 2021, pp. 359–364.
- [7] A. D. Degenhart et al., "Stabilization of a brain-computer interface via the alignment of low-dimensional spaces of neural activity," *Nature Biomed. Eng.*, vol. 4, no. 7, pp. 672–685, 2020.
- [8] M. Atzori et al., "Characterization of a benchmark database for myoelectric movement classification," *IEEE Trans. Neural Syst. Rehabil. Eng.*, vol. 23, no. 1, pp. 73–83, Jan. 2015.
- [9] X. Hu, H. Zeng, A. Song, and D. Chen, "Robust continuous hand motion recognition using wearable array myoelectric sensor," *IEEE Sensors J.*, vol. 21, no. 18, pp. 20596–20 605, Sep. 2021.
- [10] P. Esmatloo, K. Ghonasgi, R. King, and A. D. Deshpande, "Dynamic finger task identification using electromyography," in *Proc. IEEE RAS/EMBS Int. Conf. Biomed. Robot. Biomech.*, 2022, pp. 1–6.
- [11] A. Waris et al., "The effect of time on EMG classification of hand motions in able-bodied and transradial amputees," *J. Electromyogr. Kinesiol.*, vol. 40, pp. 72–80, 2018.
- [12] R. V. Schulte, E. C. Prinsen, J. H. Buurke, and M. Poel, "Adaptive lower limb pattern recognition for multi-day control," *Sensors (Basel)*, vol. 22, no. 17, 2022, Art. no. 6351.
- [13] J. He, D. Zhang, N. Jiang, X. Sheng, D. Farina, and X. Zhu, "User adaptation in long-term, open-loop myoelectric training: Implications for EMG pattern recognition in prosthesis control," *J. Neural Eng.*, vol. 12, no. 4, 2015, Art. no. 046005.
- [14] V. R. Barradas, W. Cho, and Y. Koike, "Emg space similarity feedback promotes learning of expert-like muscle activation patterns in a complex motor skill," *Front. Hum. Neurosci.*, vol. 16, 2022, Art. no. 805867.
- [15] Y. Fang, D. Zhou, K. Li, and H. Liu, "Interface prostheses with classifier-feedback-based user training," *IEEE Trans. Biomed. Eng.*, vol. 64, no. 11, pp. 2575–2583, Nov. 2017.
- [16] D. Farina et al., "The extraction of neural information from the surface emg for the control of upper-limb prostheses: Emerging avenues and challenges," *IEEE Trans. Neural Syst. Rehabil. Eng.*, vol. 22, no. 4, pp. 797–809, Jul. 2014.
- [17] J. M. Hahne, S. Dahne, H. J. Hwang, K. R. Muller, and L. C. Parra, "Concurrent adaptation of human and machine improves simultaneous and proportional myoelectric control," *IEEE Trans. Neural Syst. Rehabil. Eng.*, vol. 23, no. 4, pp. 618–627, Jul. 2015.
- [18] S. Muceli and D. Farina, "Simultaneous and proportional estimation of hand kinematics from EMG during mirrored movements at multiple degrees-of-freedom," *IEEE Trans. Neural Syst. Rehabil. Eng.*, vol. 20, no. 3, pp. 371–378, Mar. 2012.
- [19] N. Jiang, H. Rehbaum, I. Vujaklija, B. Graimann, and D. Farina, "Intuitive, online, simultaneous, and proportional myoelectric control over two degrees-of-freedom in upper limb amputees," *IEEE Trans. Neural Syst. Rehabil. Eng.*, vol. 22, no. 3, pp. 501–510, May 2014.
- [20] S. Dosen, M. Markovic, K. Somer, B. Graimann, and D. Farina, "EMG biofeedback for online predictive control of grasping force in a myoelectric prosthesis," *J. Neuroeng. Rehabil.*, vol. 12, 2015, Art. no. 55.
- [21] H. Fang et al., "Anatomically designed triboelectric wristbands with adaptive accelerated learning for human-machine interfaces," *Adv. Sci.*, vol. 10, no. 6, 2023, Art. no. e2205960.
- [22] A. Moin et al., "A wearable biosensing system with in-sensor adaptive machine learning for hand gesture recognition," *Nature Electron.*, vol. 4, no. 1, pp. 54–63, 2020.
- [23] D. Yeung, I. M. Guerra, I. Barner-Rasmussen, E. Siponen, D. Farina, and I. Vujaklija, "Co-adaptive control of bionic limbs via unsupervised adaptation of muscle synergies," *IEEE Trans. Biomed. Eng.*, vol. 69, no. 8, pp. 2581–2592, Aug. 2022.
- [24] V. Gilja et al., "A high-performance neural prosthesis enabled by control algorithm design," *Nat. Neurosci.*, vol. 15, no. 12, pp. 1752–1757, 2012.
- [25] X. Hu, H. Zeng, D. Chen, J. Zhu, and A. Song, "Real-time continuous hand motion myoelectric decoding by automated data labeling," in *Proc. IEEE Int. Conf. Robot. Autom.*, 2020, pp. 6951–6957.
- [26] M. Couraud, D. Cattaert, F. Pacllet, P. Y. Oudeyer, and A. de Rugy, "Model and experiments to optimize co-adaptation in a simplified myoelectric control system," *J. Neural Eng.*, vol. 15, no. 2, 2018, Art. no. 026006.